

Article

Rapid Access to Empirical Impact Ionization Cross Sections for Atoms and Ions across the Periodic Table

Stephan Fritzsche^{1,2,3,*} , Liguang Jiao^{1,2,4}  and Giorgio Visentin^{1,2} ¹ Helmholtz-Institute Jena, Fröbelstieg 3, 07743 Jena, Germany; g.visentin@hi-jena.gsi.de (G.V.)² GSI GSI Helmholtz Centre for Heavy Ion Research, 64291 Darmstadt, Germany³ Institute for Theoretical Physics, Friedrich-Schiller-University Jena, 07743 Jena, Germany⁴ College of Physics, Jilin University, Changchun 130012, China

* Correspondence: s.fritzsche@gsi.de

Abstract: Electron-impact ionization (EII) processes are essential for modelling high-temperature plasma in quite different research areas, from astrophysics to material science to plasma and fusion research and in several places elsewhere. In most, if not all, of these fields, partial and total EII cross sections are required, and often for a good range of electron energies, in order to determine, for instance, the level population of ions and spectral line intensities in plasma under both local and non-local thermodynamic equilibrium conditions. To obey these needs, various kinds of semi-empirical EII cross sections have been applied in practice, often simply because of the large computational demands in dealing explicitly with two free electrons within the continuum. Here, we expand JAC, the Jena Atomic Calculator, to provide such empirical EII cross sections for (most) atoms and ions across the periodic table. Five empirical models from the recent literature have been implemented to support a simple and rapid access to the partial EII cross sections for electrons from a (partly filled) shell $(n\ell)^q$ as well as the total ionization cross sections. We here restrict ourselves to the *direct* part of the EII cross section, whereas the impact excitation of electrons with subsequent autoionization and the resonant electron capture with double autoionization have been left aside in this first implementation. Rapid access to the (direct) EII cross sections will help already to better understand the role of electron-impact processes in the diagnostics of fusion plasma or the interpretation of astrophysical spectra.



Citation: Fritzsche, S.; Jiao, L.; Visentin, G. Rapid Access to Empirical Impact Ionization Cross Sections for Atoms and Ions across the Periodic Table. *Plasma* **2024**, *7*, 106–120. <https://doi.org/10.3390/plasma7010008>

Academic Editor: Andrey Starikovskiy

Received: 19 December 2023

Revised: 20 January 2024

Accepted: 23 January 2024

Published: 30 January 2024



Copyright: © 2024 by the authors. Licensee MDPI, Basel, Switzerland. This article is an open access article distributed under the terms and conditions of the Creative Commons Attribution (CC BY) license (<https://creativecommons.org/licenses/by/4.0/>).

Keywords: atoms and ions; binary-encounter approximation; electron-impact ionization; empirical model; impact ionization cross section; inner-shell ionization; Jena Atomic Calculator; partial cross section; relativistic

1. Introduction

Electron-impact ionization (EII) generally refers to the collision process of (fast) electrons with ions, atoms, molecules or the solid state, a process that is often accompanied by the relaxation of the remaining bound electrons. The impact ionization of electrons is the inverse process of three-body recombination and has been found important in many research areas, from atomic and molecular spectroscopy to astro- and plasma physics, medical science and the design of semiconductor devices. The EII process frequently occurs indeed in all (high-temperature) plasma. Apart from the *direct* ionization of bound electrons, this process formally also includes the impact excitation of target electrons with a subsequent autoionization, the resonant capture of electrons with multiple autoionization or several high-order processes in the interaction of an incoming electron with different quantum targets [1,2]. See Figure 1 for a brief overview of the various contributions to the EII process.

Of course, many of the applications above also require detailed EII cross sections. For atoms and (positively charged) ions A^{q+} in their ground configuration, the direct process $A^{q+} + e_i^- \rightarrow A^{(q+1)+*} + e_f^- + e_r^-$ first of all depends on the kinetic energy ε of

the incident (or initial) electron e_i^- , which is inelastically scattered in this process to result in a final-state electron e_f^- with energy ε_f as well as an additional (released) electron e_r^- with energy ε_r . The atom is thereby ionized and can be found either in its ground configuration or, more often than not, in some inner- or valence-shell excited level $A^{(q+1)+*}$. While various approximations (and computational methods) have been applied in the literature in order to estimate—direct and occasionally even more complete—EII cross sections [3,4], the formalisms and implementations behind them typically only have a limited range of validity and/or feasibility, and quite remarkable discrepancies may occur among different approximations [2].

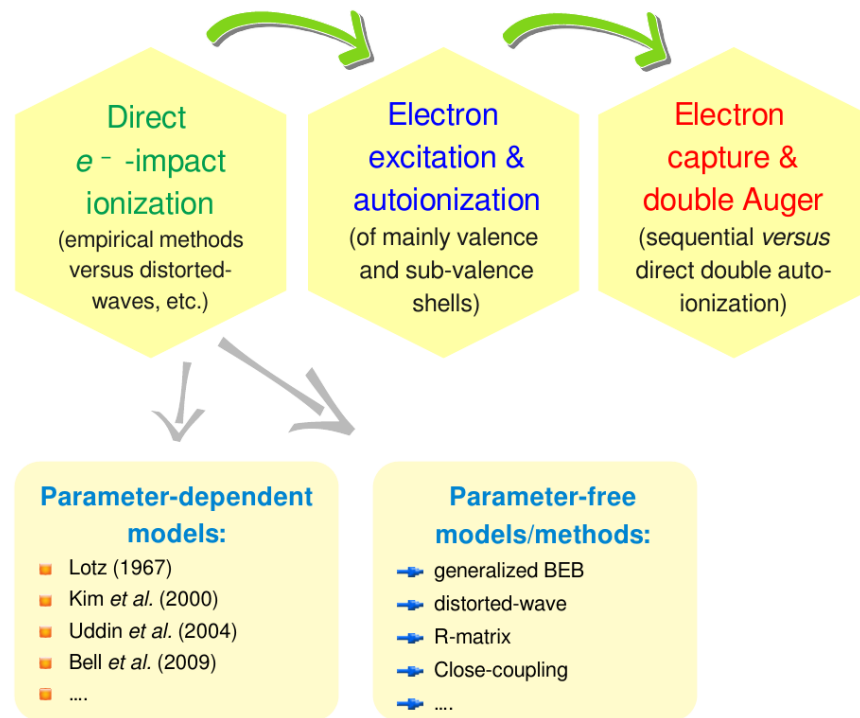


Figure 1. Overview and basic steps in the computation of partial and total EII cross sections. Apart from the direct ionization of (inner-shell) electrons by electron impact, the impact excitation of the target with a subsequent autoionization and the resonant capture of electrons with multiple autoionization or several high-order interaction processes contribute as well to the EII. Whereas most empirical models apply fit parameters, which are suitable for just one or several shells, charge states and/or elements, we here also implement a generalized and parameter-free BEB model [5]. See text for further discussion.

A number of semi-empirical models [6–8], especially the distorted-wave Born and close-coupling approximations, nowadays provide powerful quantum-mechanical methods for describing the inelastic electron scattering process from above [9,10]. However, since these methods usually come with quite high computational demands, they are still applicable only to atoms and ions with simple shell structures. Despite all the recent progress in dealing with electron–ion collision processes, therefore, a fast and reliable access to empirical EII cross sections has not yet been found indispensable for advancing research in astro- and plasma physics or elsewhere.

To provide such a rapid and reliable access to the direct—partial and total—EII cross sections, we here expand JAC, the Jena Atomic Calculator [11], to support different models for (almost) all atoms and ions from the periodic table of elements. For medium and heavy elements, moreover, a relativistic implementation of the electronic structure is required (and desirable) to model the experimentally observed level structures [12]. Unlike most other parts of JAC, these (empirical) estimates are based on just single-electron energies, typically together with a proper scaling of the (differential and) partial ionization cross

sections. Examples are shown especially for the ionization of hydrogenic Li^{2+} ions as well as for the inner-shell EII of selected ionic targets, for which the cross sections can be readily compared with data from the literature.

This study is structured as follows. In Section 2, we first recall the central assumptions and methods in treating the EII of atoms quantum-mechanically. In particular, we here outline the surmises behind the binary-encounter theory as the basic approximation behind most of the empirical models for estimating EII cross sections as functions of the impact energy ε . Section 3 then summarizes the principal features of the (five) models that are implemented within the JAC code. This includes a short account of this toolbox itself, the role of empirical computations, the definition and use of selected data structures and how all the necessary information is communicated to and within the program. The use of these additional features in JAC is later shown and explained in Section 4. For the ionization of multiply charged Ne^{8+} ions, we here demonstrate how readily the empirical model itself, the initial configuration(s), impact energies as well as the subshells of interest can be selected and specified by the user. A simple comparison of these models also enables the user to recognize and extract relativistic or inner-shell contributions to the total cross sections. Finally, a short summary and conclusions are given in Section 5.

2. Empirical Approximations for Modeling Impact Ionization Processes

2.1. Empirical Estimates versus Quantum Many-Electron Computations

In atomic physics, empirical estimates of cross sections are typically applied for the sake of feasibility and often *in contrast* to (much) more elaborate quantum many-particle computations. These estimates are mainly built upon classical arguments and combine empirical knowledge about the general energy-dependence of the EII cross sections with specific (fit) parameters that are adopted for just a single or a few selected elements. With these insights, empirical estimates can avoid many, if not all, difficulties in dealing with (quasi-)free electrons in the continuum. For the impact ionization of an (inner-shell) electron from the $(n\ell)^q$ -shell of an atom with occupation q and binding energy $\varepsilon_{n\ell}$, Lotz [13] was perhaps the first to provide empirical EII cross sections for most neutral atoms up to $Z = 108$. His well-known “Lotz formula”

$$\sigma^{(\text{EII})}(\varepsilon) = a q [10^{-14} \text{ cm}^2 \text{ eV}^2] \frac{\ln(\varepsilon/\varepsilon_{n\ell})}{\varepsilon/\varepsilon_{n\ell}} [1 - b \exp(-c(\varepsilon/\varepsilon_{n\ell} - 1))]$$

expresses the partial EII cross section for the shell $(n\ell)^q$ in terms of just three dimensionless (fit) parameters. Although this formula is no longer *state-of-the-art* in estimating EII cross sections, it reproduces a good number of measurements within about 10–20% over a wide range of impact energies, and it may still serve as a “fast educated guess” when more accurate methods are not necessary. Further improvements on this and similar empirical formulas have nowadays made the partial and total EII cross sections reliable enough for a large class of elements, charge states and impact energies, despite several (and sometimes severe) failures of these methods under certain circumstances.

Yet, serious difficulties may also occur with advanced quantum many-electron computations of EII cross sections [14]. These difficulties mainly arise from (i) missing interactions between the two outgoing electrons; (ii) a sizable, if not even large, number of relevant scattering states, owing to the coupling of the two electrons within the continuum; (iii) a δ -like normalization of free electrons (orbitals) associated with the continuous spectral part of the underlying Hamiltonian; (iv) a proper account of the boundary conditions for all in- and outgoing continuum waves as well as (v) large radial integration domains, which typically go well beyond the scope of standard (localized) atomic structure computations. In a quantum treatment of EII, each free electron formally requires a three-fold *spatial* integration up to a rather large radius (around the core) and beyond which the integration is either neglected or continued analytically. These difficulties have limited full, *ab initio* EII computations to ions with (initially) one or just a few bound electrons. For more complex shell structures, only the distorted-wave approximation appears realistic today [15–17],

in which differential (in energy) EII cross sections are obtained from the formulas of the electron-impact excitation (EIE) cross section but by replacing the excited bound electron with the second outgoing electron. Despite a good number of case studies and computations for selected ions [9,10,18], detailed cross sections are rare and still not very reliable, cf. Ref. [2].

It is this increase in (numerical) complexity that suggests and let us bring up a few empirical models of EII cross sections also within JAC, mainly by following the studies of Kim and coworkers [6,19] and related models.

2.2. Binary-Encounter Approximations

The binary-encounter (BE) approximation, as the name suggests, aims to simplify the many-electron collision into a two-body collision problem between the incident particle and just one of the bound target electrons. This approximation applies classical arguments on the shape of the differential ionization cross sections and combines them with the (classically) expected high-energy behavior. It was first developed by Thomson [20] and later expanded by Thomas [21] and Vriens [22] to quantum-mechanical collisions between identical particles, including estimates of their exchange interaction and the interference between the direct and exchange contributions. Since then, the BE approximation has been found a valuable tool in numerous applications and, in particular, if simplicity, speed or qualitative insights are needed or if a full quantum-mechanical treatment appears to be impractical.

Here, we shall not put together or explain details about the BE approximation, which has been discussed in various places [6,19]. For high impact energies, the energy-differential and dipole-allowed EII cross sections are reasonably well-described by the Bethe approximation $\sigma^{(\text{EII: Bethe})} \propto \ln E/E$, similar to the heating of matter by thermal electrons. The classical BE approximation relates the energy-differential cross section for the collision of two particles to the energy and momentum transfer among the particles. Further extensions of this approximation are known as BE-Bethe (BEB) or BE-dipole (BED) models in the literature and have lead to a number of useful formulas for partial EII cross sections for ionizing an electron from the q -fold occupied shell $(n\ell)^q$. The BED model, for instance, merges the well-known Mott cross section for the close collision of two charges with the leading dipole term from the Bethe cross section. Several of these formulas have later been expanded towards relativistic impact energies of the incident electron as well as to cover medium and heavy elements with a relativistic shell structure. In practice, however, most of these derivations have already been made with specific assumptions in mind about the behavior of the EII cross sections, and often by introducing and making use of quite sophisticated notations.

2.3. Use of Semi-Empirical Models

The need for and use of empirical EII cross sections cannot be overrated. Apart from a few rather general parameterizations of cross sections that can be applied to certain groups of atoms and ions, various special solutions have been suggested and applied in the literature in order to incorporate relativistic and ionic corrections into these cross sections [7,23–26]. For example, Vriens and Smeets [27] constructed a whole set of simple analytical formulas for EII cross sections and rate coefficients as well as for three-body recombination, even if it appears difficult to follow this paper in good detail.

Let us illustrate the use of such empirical formulas by means of the (non-relativistic) binary-encounter-dipole (BED) model. This model merges the Mott scattering for the short-range interaction of two electrons with Bethe's theory [28] in order to incorporate the (so-called) exchange and interference terms within the dipole approximation. In this model, moreover, the partial and energy-differential EII cross section for the ionization of an electron from the shell $(n\ell)^q$ is given in atomic units $[a_0^2]$ by

$$\left(\frac{d\sigma}{d\varepsilon_r}\right)^{\text{(EII: partial BED)}} = \frac{\pi a_0^2 q}{\varepsilon_{nl}^3 (t+u+1)} \left\{ \frac{N_i/q - 2}{t+1} \left(\frac{1}{w+1} + \frac{1}{t-w} \right) + \left[2 - \frac{N_i}{q} \right] \left[\frac{1}{(w+1)^2} + \frac{1}{(t-w)^2} \right] + \frac{\ln t}{q(w+1)} \frac{df}{dw} \right\}$$

$$t = \frac{\varepsilon}{\varepsilon_{nl}}, \quad u = \frac{u_{nl}}{\varepsilon_{nl}}, \quad w = \frac{\varepsilon_r}{\varepsilon_{nl}}, \quad N_i = \int_0^\infty dw \frac{df}{dw}.$$

Here, t , u , w refer to the (relative) kinetic energies of the incident, the initially bound and, respectively, the finally released electron, all normalized with regard to the binding energy ε_{nl} of the ionized electron. Moreover, $\frac{df}{dw} = \varepsilon_{nl} \frac{df}{d\varepsilon_r} \propto \varepsilon_{nl} \sigma^{(PI)}(\omega)$ denotes the (so-called) differential dipole oscillator strengths [29]. This and similar formulas can be found in the literature, although often expressed using rather tedious notations. All the (relative) energies and parameters in these formulas are readily available from atomic structure codes; of course, they could also be refined by taking empirical data from the literature, but for the price that these energies need first to be collected and evaluated critically. For large impact energies ε of the incident electrons, furthermore, several corrections have been introduced and discussed as well in the differential EII cross sections, which may then lead to sizable, though realistic, enhancements. At incident electron energies $\varepsilon \approx 300$ keV, the relativistic contributions can double the total EII cross section of H and He, and they will become dominant at even higher energies.

Today, a good number of such binary-encounter-type models are known from the literature with various more-or-less useful improvements, corrections and empirical scalings for selected elements and shell structures [7,23–26]. No attempt is made here to carefully evaluate, compare or analyze these models in further detail. In the implementation below, we instead have chosen five recently refined and applied models in order to help users with a simple and rapid access to the direct EII cross sections. Indeed, the main emphasis has been placed on a simple use of these cross sections, while the accuracy of data cannot always be ensured and (may) requires a comparison with ab initio data (if available) or other information from the literature. These models should be applicable quite independent of the given element, its charge state and shell structure, even if these simple requests will not be fulfilled by all these models equally. Table 1 summarizes a few central features and limitations of the selected models as well as the associated (concrete) data type `<: ImpactIonization.AbstractModel` that help select a particular model within the code [cf. Section 3.2 below]. All these models incorporate various modifications with regard to the original BEB and BED cross sections and can be applied to (certain groups of) multiply charged ions as well as to the impact ionization of neutral atoms. The use of some relativistic model is typically suggested for all impact energies $\varepsilon \gtrsim 50$ keV as well as for the inner-shell ionization of heavy atoms and ions with, say, $Z \gtrsim 70$. Whereas the (non-relativistic) BEB and BED models can be applied to all shells of light or medium atoms, though with a different numerical uncertainty, the parameter-dependent BED model of Haque and coworkers [8,30] has been designed especially for the partial K-, L- and M-shell EII cross sections of medium-Z elements. Moreover, the partial EII cross sections are usually less accurate for the direct impact ionization of valence shells owing to their low binding energies and their sensitivity to missing correlations.

Table 1. Empirical models for the EII of atoms and ions that are implemented in the JAC toolbox. For each of these models, we here recall a few central features, major limitations and the associated concrete data type <: `ImpactIonization.AbstractModel`, which is taken to select a particular model internally.

Model	Features and Limitations
Generalized binary-encounter Bethe (BEB):	suitable for non-relativistic and relativistic impact energies and most not-too-heavy elements. This model is parameter-free and easy to use [5] and expands the EII cross sections of Kim and coworkers [6,19]. It is often applied to light and medium elements with $Z \lesssim 30$, as well as to the EII of (sub-)valence shells. The relativistic version of this model is suggested for impact energies $\varepsilon \gtrsim 50$ keV; <code>ImpactIonization.BEBmodel</code> , <code>ImpactIonization.RelativisticBEBmodel</code> .
Binary-encounter-dipole (BED):	a modified BEB model following the studies of Huo [31] and Uddin and coworkers [32]. Again, this model is suitable for both non-relativistic and relativistic impact energies, but is based especially on fit parameters; <code>ImpactIonization.BEDmodel</code> , <code>RelativisticBEDmodel</code> .
Parameter-dependent (fitted) BED:	another modified BEB model due to Haque and coworkers [8,30]. This model can be applied to a good range of impact energies by making use of different fit coefficients for the K-, L- and M-subshells. It incorporates certain ionic and relativistic corrections and has been applied successfully up to ultra-high energies $\varepsilon \leq 2$ GeV for atomic targets with nuclear charge $Z = 1, \dots, 92$; <code>ImpactIonization.FittedBEDmodel</code> .

2.4. Resonant Excitation and Capture Contributions to Electron-Impact Ionization

Whereas the direct ionization process typically contributes most to the (total) impact ionization cross section, it does not describe the EII process completely. Other non-resonant contributions arise from the excitation of inner-shell electrons and their subsequent autoionization. Here, the initial excitation step first brings the ion into the continuum of the next (or even several) higher charge state and, hence, makes autoionization of the atom possible. Of course, any inner-shell excitation $A^{q+} + e_i^- \rightarrow A^{q+(*)} + e_f^- \rightarrow A^{(q+1)+*} + e_f^- + e_r^-$ comes with a well-defined threshold in the impact energy of the incident electrons. The same final state of the ion can usually also be reached by some resonant electron capture and either sequential or double autoionization: $A^{q+} + e_i^- \rightarrow A^{(q-1)+(*)} \rightarrow A^{(q+1)+*} + e_f^- + e_r^-$. These resonant contributions to the EII cross sections are sometimes referred to as resonant-capture double autoionization (RCDA) and resonant-capture Auger double ionization (RCADI), respectively. In practice, however, the inner-shell excitation and resonant-capture contributions can both be implemented more readily in atomic-structure theory by means of atomic cascades [33,34], since they require the computation of many electron transition amplitudes for different processes, such as for an impact excitation, autoionization or the dielectronic capture of atoms and ions; cf. Ref. [35–37].

In particular, the (inner-shell) excitation-with-autoionization contributions to the partial EII cross section are known to become significant for impact energies for which the valence-shell ionization is still dominant. Until the present, this excitation with autoionization has been considered in the literature for selected ions only [38,39]. To deal with these contributions, we have recently restructured the code for cascade computations in JAC in order to support (in the foreseeable future) such non-resonant and resonant contributions within EII cross sections [40].

3. Implementation of Partial and Total Electron-Impact Cross Sections

With this short account of empirical estimates of EII cross sections for atoms and ions, let us now expand JAC, the Jena Atomic Calculator, to make use of the selected models [cf. Table 1] and to facilitate their rapid access and comparison. To this end, we have introduced the concept of `Empirical.Computation` as a new and efficient tool in order to deal with a good number of empirical models and estimates.

3.1. The JAC Toolbox

JAC was originally developed as a platform to support atomic structure calculations of different kinds and complexity for many atoms and ions, including level energies, energy shifts, rates and cross sections for a large variety of atomic processes and experimental scenarios [11]. A primary goal in designing this platform was to establish a general and easy-to-use toolbox that integrates different physical and computational demands within a single framework and, thus, to help ensure good self-consistency of all generated data. With the implementation of JAC, we also aim to provide a descriptive language that (i) emphasizes the underlying atomic physics, (ii) facilitates both a seldom and more frequent use of this toolbox and (iii) avoids most technical slang common to many atomic structure codes [41]. An overview about the JAC toolbox has been given elsewhere, along with a link to download the code [42].

Our implementation of JAC makes use of Julia as a new language for scientific computing. This programming language embraces as number of (modern) features, such as abstract and dynamic types, optional type annotations, type-specializing, just-in-time compilation of code and dynamic code loading or garbage collection, to name just a few [43,44]. It has been designed as a functional language where procedures serve as basic “words and idioms” in order to operate upon data types and/or data structures and to fulfill well-defined tasks. When compared with other programming languages, Julia’s type system, and particularly its abstract data types, helps establish a hierarchy of relationships between data and actions and, hence, to model *behavior* within large code projects. Since Julia is built by default on *dynamic* arrays, whose size can simply grow by pushing further data to it, this computing language enables one to arrange and clearly articulate data in a form suitable for solving complex tasks in physics [45]. In addition, Julia also includes powerful features for *parallelization*.

Until the present, JAC’s (so-called) `Atomic.Computation` has been one of its central data types to describe and control the calculation of atomic properties, processes and cascades [40]. This data type is typically based on a list of explicitly given electron configurations in order to generate all atomic state functions of interest and to provide a simple communication and interface between the different parts of the program. In this contribution, we here expand JAC to also support a few `Empirical.Computations` for obtaining (total) energies and cross section estimates, mainly based on empirical arguments and algorithms.

During the past years, JAC has been sizeably enlarged along different lines both to assist “additional” physics computations and to make the code more readily accessible to users. Apart from calculating the electronic structure and properties of free atoms and ions, the focus in JAC’s development was placed on the treatment of open *f*-shell elements [46], the computations of radiative and dielectronic recombination plasma rate coefficients [47,48], the setup of approximate Green functions [49], the algebraic evaluation of expressions from Racah’s algebra [50] and even estimating atomic (line) energies and decay rates under different plasma environments [51]. We here follow similar objectives, as summarized above, by adding features to JAC for providing useful empirical estimates of the partial and total EII cross sections.

3.2. Empirical Estimates of EII Cross Sections within JAC

Empirical estimates of atomic data and cross sections are useful (and needed) if detailed quantum computations either are impractical or appear unfeasible. Examples of such empirical data include certain excitation and decay energies of inner-shell excited (hole) configurations, for instance, in terms of the (one-electron) Dirac–Fock binding energies, atomic radii, polarizabilities of ionic ground levels, ionization and charge-exchange cross sections or, perhaps more challenging, ion mobilities and stopping powers in buffer gases or thin foils. To deal with these and similar (empirical) estimates, we have defined and here apply the data structure `Empirical.Computation` in order to handle different entities, models and/or data sets. These estimates can then also be used internally in JAC or as

input to other codes for describing, possibly, the radiation transfer or ionization balance in a plasma.

In practice, the data type `Empirical.Computation` is quite simple to employ. The lower panel of Figure 2 displays its internal definition which, apart from a short name, just comprises information about the nuclear charge (model), a radial grid if needed as well as a list of electron configurations. These configurations describe the shell occupation of the underlying atom or ion, whose electronic structure is later, however, treated by its *mean* charge distribution and the associated one-electron spectrum. For these configurations, an atomic mean-field representation is first generated in order to obtain the electron binding and kinetic energies for all shells ($n\ell$) of the given system. From the binding energies, we can also determine the effective charge that is felt by an electron in the given subshell and which enters, for instance, the generalized BEB model [5]. The current property of interest in such empirical computations is selected by means of the `settings::Basics.AbstractEmpiricalSettings`, which enable the user to distinguish between the different branches of these tools; cf. the upper panel of Figure 2 for the definition of this abstract type, which ensures internally the dynamic assignment of the correct code. Of course, each empirical computation also leads to a rather specific outcome that is typically returned in some dictionary (structure), along with a proper printout to screen.

```

abstract type Basics.AbstractEmpiricalSettings
... defines an abstract type to distinguish between and to deal with different settings
of empirical processes/computations.

struct Empirical.Computation
... defines a type for the empirical estimation of (total) energies as well cross sections
for various ionization and charge exchange processes.

+ name           ::String           ... A name associated to the given computation.
+ nuclearModel   ::Nuclear.Model     ... Model, charge and parameters of the nucleus.
+ grid           ::Radial.Grid       ... The radial grid to be used in the computations.
+ configs        ::Array{Configuration,1} ... A list of non-relativistic configurations.
+ settings       ::Basics.AbstractEmpiricalSettings
... Provides the settings for the selected kind of computations (estimates).

```

Figure 2. Definition of the data structure `Empirical.Computation` that helps support quick estimates of different properties in JAC. See Section 3.2 for further explanations.

Table 1 displays the five empirical models that have been implemented in JAC. For each of these models, this table lists a few central features and limitations that apply with regard to the impact energy ε , the range of atoms or ions and the types of cross sections that can be estimated. It shows the concrete data type `Model <: ImpactIonization.AbstractModel`, which helps select a particular model and strengthens the control of the program; cf. the upper panel of Figure 3. The use of an abstract type also allows the user to readily add new and modified approximations without other parts of the program needing to be altered.

Apart from this (abstract) type, Figure 3 displays two relevant data types that help estimate EII cross sections based on some particular empirical model. In fact, all further information and control parameters are provided by the settings of the `Empirical.Computation` and will make the implementation of further properties straightforward. In these settings, we provide the selected model, the impact energies ε , the selected shells (middle panel of Figure 3) as well as a number of logical flags to distinguish between the partial and total cross sections. A more detailed description of these data types can also be obtained interactively, for instance, with `? ImpactIonization.BEBmodel`, to recall the purpose of this struct and the definition of all subfields. In total, there are at present about 250 of these data structures in JAC, although most of them remain hidden from the user.


```

abstract type ImpactIonization.AbstractModel
... defines an abstract and a number of (concrete= singleton types for the computation of
empirical EII cross sections in different models.

+ struct BEBmodel
... to apply a generalized binary-encounter Bethe (BEB) model for non-relativistic impact
energies; cf. Kim et al (2001) and Wang et al (2023).
+ struct BEDmodel
... to apply the binary-encounter dipole BED model due to Huo, PRA (2001) for non-relativistic
impact energies.
+ struct RelativisticBEBmodel
... to apply a generalized relativistic BEB model for relativistic impact energies
(Wang et al., 2023).
+ struct RelativisticBEDmodel
... to apply a modified relativistic BED model due to Uddin et al. PRA (2005) for
relativistic impact energies.
+ struct FittedBEDmodel
... to apply a modified relativistic BEB model due to Haque et al. AQC (2017) for both,
non-relativistic & relativistic impact energies, and by using fitting coefficients
for the K-, L-, and M-subshells (sometimes also known as MUIBED in the literature).

struct Basics.ShellSelection
... defines a struct to specify a list of shells by means of different constructors.

+ active      ::Bool           ... true, if some selection has been made.
+ shells      ::Array{Shell,1} ... List of explicitly selected shells.
+ lSymmetries ::Array{Int64,1} ... List of selected (partial-wave) l-symmetries.

struct ImpactIonization.Settings <: AbstractEmpiricalSettings
... defines a type for the settings of (calculating) empirical electron-impact ionization
cross sections.

+ model              ::ImpactIonization.AbstractModel
... The particular model to be used for the empirical EII cross sections.
+ impactEnergies     ::Array{Float64,1}
... List of impact-energies of the incoming electrons [in user-specified units].
+ calcPartialCs      ::Bool
... True if partial (shell-dependent) cross sections are to be calculated, and false otherwise.
+ calcTotalCs        ::Bool
... True if total cross sections are to be calculated, and false otherwise.
+ shellSelection     ::ShellSelection
... Provides the selected shells for the computation of partial EII cross sections, if any.

```

Figure 3. Abstract and concrete data types in JAC that help estimate partial and total EII cross sections by applying different empirical models for given impact energies as well as for impact ionization from selected shells. See text for further explanations.

4. Rapid Access to and Comparison of EII Cross Sections from Different Models

4.1. K-Shell Electron-Impact Ionization of Ne^{8+} Ions

Measurements of (partial) K-shell EII cross sections have a long tradition in the literature [52–54]. The ionization of these K-shell electrons can be readily detected for most medium and heavy elements by just recording the subsequent X-ray emission, which, on its own, has been utilized in a good number of applications. In thermal plasma, for example, the electron-impact ionization of atoms or ions governs the evolution of the ion charge state distribution. While the target atoms are often simply irradiated WITH some electron gun, the emitted X-rays are usually observed by means of semiconductor detectors. In practice, most EII cross section measurements have been restricted to impact energies of about $\varepsilon \lesssim 10\text{--}50$ keV.

For Ne^{q+} ($q = 1, \dots, 9$) ions, in particular, the K-shell EII cross sections have been deduced from the analysis of the charge state distribution evolution of ions that were extracted from an electron-beam ion source for high impact energies $\varepsilon = 2.7\text{--}10.0$ keV [53]. These ions are relevant because neon has frequently been utilized in tokamaks as a diagnostic element for probing fusion plasmas [55]. To provide a quick estimate of the K-shell EII cross sections for just helium-like Ne^{8+} ions, Figure 4 shows the (Julia) input that needs to be prepared by the user to apply the JAC toolbox. Apart from selecting the units of all (one-electron) energies at in- and output times, this input script specifies a name (string), the nuclear model and a radial grid, as appropriate for a mean-field representation of the given ion, as well as its ground configuration, from which the impact ionization takes place. In the

settings, moreover, we call for cross sections for the input energies $iEnergies = [1200., 1600., 2000., \dots]$ eV. Obviously, moreover, we can only include the ionization from the 1s shell for helium-like ions, where the partial and total EII cross sections will coincide in this case. All the cross sections are eventually printed to screen once the computations have been performed. Let us mention, finally, that all these calls in Figure 4 can also be made line-wise in order to immediately see and check the consistency of the given specifications.

```
# Calculate partial K-subshell EII cross section of Ne8+ in different models;
# choose one of BEBmodel(), BEDmodel(), RelativisticBEBmodel(), RelativisticBEDmodel(),
# FittedBEDmodel().
setDefault("unit: energy", "eV")
model      = ImpactIonization.RelativisticBEBmodel()
name       = "EII cross section for K-subshell of Ne8+."
nucModel   = Nuclear.Model(10.0)
grid       = Radial.Grid(Radial.Grid(true), rbox = 3.0)
iEnergies  = [1200., 1600., 2000., 4000., 6000., 10000., 20000., 60000., 100000.] # [eV].
selection  = ShellSelection(true, [Shell("1s")], Int64[])
configs    = [Configuration("1s2")]
eiiSettings = ImpactIonization.Settings(model, iEnergies, true, false, selection)
comp       = Empirical.Computation(name, nucModel, grid, configs, eiiSettings)
#
perform(comp)
```

Figure 4. Input to the JAC toolbox for estimating K-shell EII cross sections for helium-like Ne⁸⁺ ions by means of generalized (relativistic) BEB model. Other models can be readily selected as well. Once the computations are performed, the partial and total resonance strengths are printed to screen for all selected (sub)shells. See text for further discussions.

Figure 5 compares the partial EII cross sections for the ionization of a K-shell electron of helium-like Ne⁸⁺ ions obtained from different computations and measurements. The results are shown for impact energies from the threshold $\varepsilon_{\text{thr}} \approx 0.6 \leq \varepsilon \lesssim 100$ [keV]. In particular, cross section estimates from the JAC toolbox in the generalized BEB model (BEBmodel()); solid black line) are compared with the estimates of Haque and coworkers ([52]; green dashed-dotted line) and the measurements of Duponchelle et al. ([56]; red squares) as well as those of Donets and Ovsyannikov ([53]; black circles). After a rather steep rise in the cross section up to its maximum just below $\varepsilon \approx 4000$ eV, the cross section smoothly decreases, typical for high impact energies. Good agreement is found, especially with the experiments of Duponchelle et al. [56], even if these experimental data might still be affected by ions in the metastable $1s2s\ ^{1,3}S$ levels. Besides the K-shell EII cross section in Figure 5, these authors have also reported double ionization for $q = 5$ and 6.

Predictions of the K-shell EII cross sections have been found sensitive, especially for low-Z atoms and ions. By using a similar input as in Figure 4, we have also estimated the 1s ionization of hydrogen-like Li²⁺ ions at low impact energies $\varepsilon \gtrsim 0.14$ keV. Figure 6 displays and compares the partial cross sections from the generalized BEB model with the original BEB estimates of Kim and Rudd [24] and the measurements by Tinschert et al. [57]. For these low-Z ions, the use of an effective charge in the generalized BEB is crucial and brings the estimated cross sections in close agreement with the experiment. Whereas such computations are obviously selective and cannot ensure the same accuracy for the EII cross sections of all other atoms and ions, a comparable good agreement has been found in a number of further test calculations.

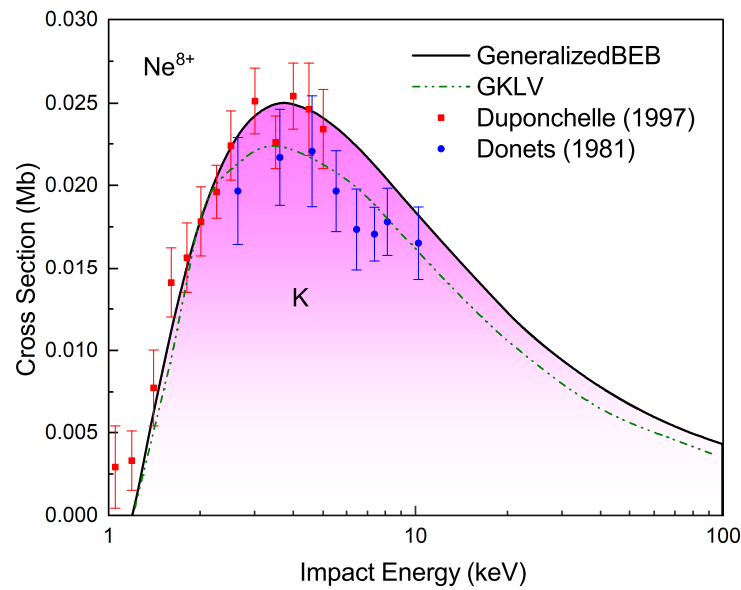


Figure 5. K-shell EII cross sections $\sigma_K^{(EII)}(\epsilon)$ for helium-like Ne^{8+} ions. Cross-section estimates from the JAC toolbox in the generalized relativistic BEB model (`RelativisticBEBmodel()`), cf. Table 1; black solid line) are compared with estimates by Haque and coworkers ([52], green dashed-dotted line) as well as measurements by Duponchelle et al. ([56], red squares) and Donets and Ovsyannikov ([53], blue circles).

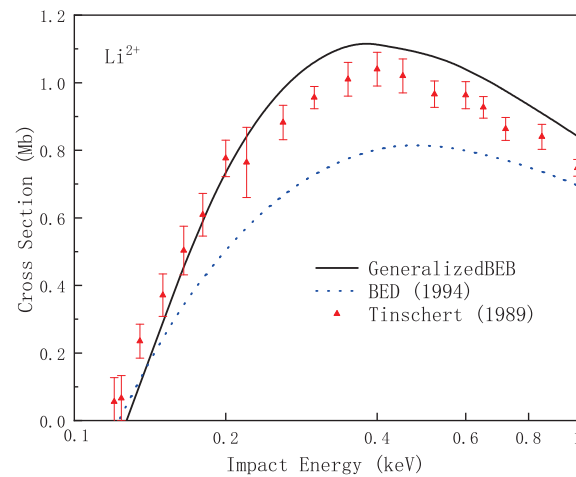


Figure 6. K-shell EII cross sections $\sigma_K^{(EII)}(\epsilon)$ for hydrogen-like Li^{2+} ions. Partial cross sections from the generalized BEB model (`BEBmodel()`; black solid line) are compared with the original BEB estimates (blue dashed line) of Kim and Rudd [24] and the measurements of Tinschert et al. ([57]; red triangles).

4.2. Partial M-Shell and Total EII Cross Sections for Argon-like Kr^{18+} Ions

Multiply charged krypton ions have been proposed as candidate for the plasma diagnostics of future thermo-nuclear reactors. The spectroscopy of these ions may help deduce the plasma temperature, both in the central region and at the edges of fusion devices. Under these conditions, however, the ions often populate not only the ground but also several (metastable) excited levels.

With JAC, we can follow similar lines as in Figure 4 above. Instead of the single 1s shell, we here consider the impact ionization from the 1s, 2s, 2p, 3s and 3p shells for argon-like Kr^{18+} ions ($Z = 36$) in their $[\text{Ar}] \equiv 1s^2 2s^2 2p^6 3s^2 3p^6$ ground configuration. We also adopt the impact energies `iEnergies = [en^1.3 for en=0.5:36.0]` to ensure a smooth behavior of the generated partial and total cross sections in the plot. All further input can

be chosen analogously to Figure 4 and independent of the particular model that is applied in the empirical estimation. Figure 7 shows the partial and total EII cross sections of the Kr^{18+} ions for impact energies $0.5 < \varepsilon \lesssim 100$ keV. The partial cross sections for the K-, L- and M-subshells (Figure 7a) have been calculated in the generalized BEB model and are distinguished by color, whereas the total EII cross section (black solid line) from the present work is compared with similar estimations by Haque and coworkers ([52]; green dashed line) as well as the measurements by Khouilid et al. ([58]; red circles). Figure 7b compares the partial M_3 EII cross sections from three different models implemented in the JAC toolbox. The estimates from these models can be readily obtained by selecting a proper Model <: AbstractModel in the input script and differ by about 15% from each other, with some favor for the generalized BEB model (BEBmodel). In these computations, all relative energies are applied, as obtained from a simple mean-field computation of the ionic ground configuration.

The total EII cross sections can be compared with the measurements by Khouilid et al. [58], who applied the animated crossed-beam method for all Kr^{q+} ($q = 12\text{--}18$) ions in the energy range from threshold to about 5.5 keV. In their setup, metastable states may have contributed as well to the cross sections for Kr^{18+} ions, besides their 1S_0 ground level. These measurements also show that at low impact energies, the inner-shell excitation of the $2s + 2p$ (and to a minor extent, the $1s$) shells plays a relevant role owing to the rapid autoionization of these hole configurations. These inner-shell excitation also explains the various “jumps” in the total EII cross section in terms of the excitation thresholds and the contributions from the different shells [59]. The role of these excitation–autoionization processes is also seen in the rather large deviations of all empirical models for impact energies below and near the maximum of the total cross section. Similar measurements have been performed for other krypton ions [60] based on Hartree–Fock threshold energies [61].

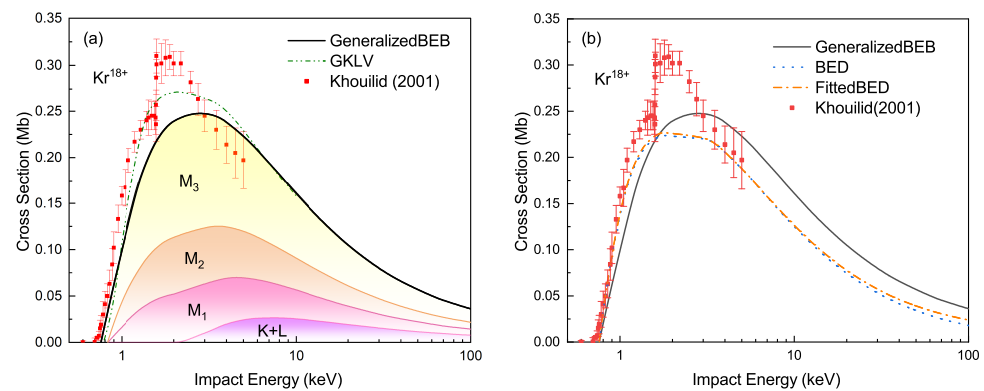


Figure 7. K-, L- and M-shell partial EII cross sections of the Kr^{18+} ions for impact energies $\varepsilon = 0.6\text{--}100$ keV. (a) The partial cross sections from the generalized BEB model are shown in color for the individual (sub)shells, while the total EII cross section (black solid line) from the present work is compared with the estimates of Haque and coworkers ([52], green dashed line) and the measurements by Khouilid et al. ([58], red circles). The jumps in the measured EII cross sections (red circles) at $\varepsilon \approx 1.5$ keV arise from the onset of $2p \rightarrow 3d$ electron-impact excitations with subsequent autoionization. (b) Comparison of the M_3 partial EII cross section from four empirical models implemented in JAC: generalized BEBmodel (black solid line), BEDmodel (green dashed line) and FittedBEBmodel (red dashed-dotted line); cf. Table 1 for a brief account of these empirical models.

5. Summary and Outlook

Reliable (direct) EII cross sections are indeed crucial for many applications in astro- and plasma physics and in various other places. This work demonstrates how readily partial and total EII cross sections can be estimated for most atoms and ions without further information and parameters needing to be provided. Emphasis has been placed especially on a rapid access and comparison of these EII cross sections as predicted by different

models. All estimates are just based on the (relative) single-shell energies, easily obtained from atomic mean-field computations. In order to support a simple use of these estimates, we, moreover, have introduced `Empirical.Computation` into JAC, which helps comprise and control all necessary input, such as the (ground) configuration of the atom or ion, the range of impact energies or the (sub)shells for which the partial cross sections need to be determined. The implementation in JAC also enables one to easily account for relativistic contributions in the EII cross sections.

Partial EII cross sections from JAC's present expansion are shown for the ionization of both inner- and valence-shell electrons. Apart from the obvious success of the given estimates and their good agreement with experiments, care should be taken for low- Z atoms and ions, for which advanced quantum computations are available [4]. While the empirical computations above deal first of all with the *direct* part of these cross sections, we also plan to implement future (cascade) computations [40] for the resonant excitation with subsequent autoionization and/or the (resonant) capture with subsequent double ionization. In practice, however, the present tools already offer useful features for the computation of level populations and spectral line intensities of non-LTE plasmas. In addition, they might be found useful for plasma diagnostics and the simulation of light curves from neutron-star mergers and other multi-messenger events.

Author Contributions: Methodology, S.F., L.J. and G.V.; software, S.F.; writing—review and editing, S.F., L.J. and G.V. All authors have read and agreed to the published version of the manuscript.

Funding: This research received no external funding.

Institutional Review Board Statement: Not applicable.

Informed Consent Statement: Not applicable.

Data Availability Statement: The data in Figures 5–7 can be reconstructed by means of the JAC toolbox, provided at the website [42].

Acknowledgments: We are grateful to Yuancheng Wang for many discussions and the implementation of the partial cross sections in the JAC toolbox.

Conflicts of Interest: The authors declare no conflicts of interest.

References

1. Burgess, A.; Chidichimo, M.C. Electron impact ionization of complex ions. *Mon. Not. R. Astro. Soc.* **1983**, *203*, 1269. [[CrossRef](#)]
2. Märk, T.D.; Dunn, G.H. (Eds.) *Electron Impact Ionization*; Springer Science & Business Media: Berlin/Heidelberg, Germany, 2013.
3. Bartlett, P.L.; Stelbovics, A.T. Calculation of electron-impact total-ionization cross sections. *Phys. Rev. A* **2002**, *66*, 012707. [[CrossRef](#)]
4. Bartlett, P.L.; Stelbovics, A.T. Electron-impact ionization cross sections for elements $Z = 1$ to $Z = 54$. *At. Data Nucl. Data Tables* **2004**, *86*, 235. [[CrossRef](#)]
5. Wang, Y.-C.; Jiao, L.G.; Fritzsche, S. Generalized binary-encounter-Bethe model for electron impact ionization of atoms. *J. Phys. B* **2023**, *accepted*.
6. Kim, Y.K.; Santos, J.P.; Parente, F. Extension of the binary-encounter-dipole model to relativistic incident electrons. *Phys. Rev. A* **2000**, *62*, 052710. [[CrossRef](#)]
7. Uddin, M.A.; Haque, A.K.F.; Billah, M.M.; Basak, A.K.; Karim, K.R.; Saha, B.C. Computation of electron-impact K-shell ionization cross sections of atoms. *Phys. Rev. A* **2005**, *71*, 032715. [[CrossRef](#)]
8. Haque, A.K.F.; Uddin, M.A.; Shahjahan, M.; Talukder, M.R.; Basak, A.K.; Saha, B.C. Electron impact inner-shell ionization of atoms. *Adv. Quantum Chem.* **2011**, *61*, 317.
9. Bartschat, K.; Burke, P.G. The R-matrix method for electron impact ionisation. *J. Phys. B* **1987**, *20*, 3191. [[CrossRef](#)]
10. Pindzola, M.S.; Schultz, D.R. Time-dependent close-coupling method for electron-impact ionization of hydrogen. *Phys. Rev. A* **1996**, *53*, 1525. [[CrossRef](#)]
11. Fritzsche, S. A fresh computational approach to atomic structures, processes and cascades. *Comp. Phys. Commun.* **2019**, *240*, 1. [[CrossRef](#)]
12. Grant, I.P. *Relativistic Quantum Theory of Atoms and Molecules: Theory and Computation*; Springer: Berlin/Heidelberg, Germany, 2007.
13. Lotz, W. Electron-impact ionization cross-sections for atoms up to $Z = 108$. *Z. Phys.* **1970**, *232*, 101. [[CrossRef](#)]
14. Bartlett, P.L.; Stelbovics, A.T. Electron-helium S-wave model benchmark calculations. I. Single ionization and single excitation. *Phys. Rev. A* **2010**, *81*, 022715. [[CrossRef](#)]

15. Younger, S.M. Distorted-wave electron-impact-ionization cross sections for highly ionized neonlike atoms. *Phys. Rev. A* **1981**, *23*, 1138. [[CrossRef](#)]
16. Griffin, D.C.; Pindzola, M.S. Distorted-wave calculations of electron impact ionisation in the Ni isonuclear sequence. *J. Phys. B* **1988**, *21*, 3253. [[CrossRef](#)]
17. Badnell N.R. A Breit-Pauli distorted wave implementation for AUTOSTRUCTURE. *Comp. Phys. Commun.* **2011**, *182*, 1528. [[CrossRef](#)]
18. Mao, J.; Badnell, N.R.; Del Zanna, G. R-matrix electron-impact excitation data for the C-like iso-electronic sequence. *Astron. Astrophys.* **2020**, *634*, A7. [[CrossRef](#)]
19. Kim, Y.-K. Scaling of plane-wave Born cross sections for electron-impact excitation of neutral atoms. *Phys. Rev. A* **2001**, *64*, 032713. [[CrossRef](#)]
20. Thomson, J.J. XLII. Ionization by moving electrified particle. *Lond. Edinb. Dublin Philos. Mag. J. Sci.* **1912**, *23*, 449. [[CrossRef](#)]
21. Thomas, L.H. The calculation of atomic fields. *Proc. Camb. Phil. Soc.* **1927**, *73*, 713. [[CrossRef](#)]
22. Vriens, L. Binary-encounter proton-atom collision theory. *Proc. Phys. Soc.* **1967**, *90*, 935. [[CrossRef](#)]
23. Kolbenstvedt, H. Simple theory for K-Ionization by relativistic electrons. *J. Appl. Phys.* **1967**, *38*, 4785. [[CrossRef](#)]
24. Kim, Y.K.; Rudd, M.E. Binary-encounter-dipole model for electron-impact ionization. *Phys. Rev. A* **1994**, *50*, 3954. [[CrossRef](#)]
25. Bell, K.L.; Gilbody, H.B.; Hughes, J.G.; Kingston, A.E.; Smith, F.J. Recommended data on the electron impact ionization of light atoms and ions. *J. Phys. Chem. Ref. Data* **2008**, *41*, 095204. [[CrossRef](#)]
26. Guerra, M.; Parente, F.; Indelicato, P.; Santos, J.P. Modified binary encounter Bethe model for electron-impact ionization. *Int. J. Mass Spectrom.* **2012**, *1–7*, 313. [[CrossRef](#)]
27. Vriens, L.; Smeets, A.H.M. Cross-section and rate formulas for electron-impact ionization, excitation, deexcitation and total depopulation of excited atoms. *Phys. Rev. A* **1980**, *22*, 940. [[CrossRef](#)]
28. Bethe, H. Zur Theorie des Durchgangs schneller Korpuskularstrahlen durch Materie. *Ann. Phys.* **1930**, *5*, 325. [[CrossRef](#)]
29. Gallagher, J. Absolute cross sections for molecular photoabsorption, partial photoionization, and ionic photofragmentation processes. *J. Phys. Chem. Ref. Data* **1988**, *17*, 9. [[CrossRef](#)]
30. Patoary, M.A.R.; Haque, A.K.F.; Hossain, M.I.; Hosain, M.E.; Uddin, M.A.; Basak, A.K.; Haque, M.M.; Maaza, M.; Saha, B.C. An analytical model for the electron impact K-shell ionization cross sections of atoms. *Int. J. Mass Spec.* **2017**, *415*, 1. [[CrossRef](#)]
31. Huo, W.M. Convergent series representation for the generalized oscillator strength of electron-impact ionization and an improved binary-encounter-dipole model. *Phys. Rev. A* **2001**, *64*, 042719. [[CrossRef](#)]
32. Uddin, M.A.; Fazlul Haque, M.A.K.; Basak, A.K.; Saha, B.C. Calculations of electron-impact single-ionization cross sections of helium isoelectronic systems. *Phys. Rev. A* **2004**, *70*, 032706. [[CrossRef](#)]
33. Schippers, S.; Martins, M.; Beerwerth, R.; Bari, S.; Holste, K.; Schubert, K.; Viehhaus, J.; Savin, D. W.; Fritzsche, S.; Müller, A. Near L-edge single and multiple photoionization of singly charged iron ions. *Astrophys. J.* **2017**, *849*, 5. [[CrossRef](#)]
34. Beerwerth, R.; Buhr, T.; Perry-Sassmannshausen, A.; Stock, S.O.; Bari, S.; Holste, K.; Kilcoyne, A.L.D.; Reinwardt, S.; Ricz, S.; Savin, D.W.; et al. Near L-edge single and multiple photoionization of triply charged iron ions. *Astrophys. J.* **2019**, *887*, 189. [[CrossRef](#)]
35. Sharma, L.; Surzhykov, A.; Srivastava, R.; Fritzsche, S. Electron-impact excitation of singly charged metal ions. *Phys. Rev. A* **2011**, *83*, 062701. [[CrossRef](#)]
36. Wu, Z.W.; Tian, Z.Q.; Dong, C.Z.; Surzhykov, A.; Fritzsche, S. Hyperfine-induced effects on $K\alpha_1$ linear polarization following electron-impact excitation of helium-like Tl^{79+} ions with nuclear spin. *I = 1/2 New J. Phys.* **2023**, *25*, 093039. [[CrossRef](#)]
37. Fritzsche S. The RATIP program for relativistic calculations of atomic transition, ionization and recombination properties. *Comp. Phys. Commun.* **2012**, *183* 1525. [[CrossRef](#)]
38. Pindzola, M.S.; Griffin, D.C.; Botcher, C. Electron-impact excitation autoionization of Ga II. *Phys. Rev. A* **1982**, *25*, 211. [[CrossRef](#)]
39. Pakalka, S.; Kucas, S.; Masys, S.; Kyniene, A.; Momkauskaite, A.; Jonauskas, V. Electron-impact single ionization of the Se^{3+} ion. *Phys. Rev. A* **2018**, *97*, 012708. [[CrossRef](#)]
40. Fritzsche, S.; Palmeri, P.; Schippers, S. Atomic cascade computations. *Symmetry* **2021**, *13*, 520. [[CrossRef](#)]
41. Fritzsche, S. Application of symmetry-adapted atomic amplitudes. *Atoms* **2022**, *10*, 127. [[CrossRef](#)]
42. Fritzsche S. JAC: User Guide, Compendium & Theoretical Background. Available online: <https://github.com/OpenJAC/JAC.jl> (accessed on 10 December 2023).
43. Available online: <https://docs.julialang.org> (accessed on 10 December 2023).
44. Bezanson, J.; Chen, J.; Chung, B.; Karpinski, S.; Shah, V.B.; Vitek, J.; Zoubritzky, J. Julia: Dynamism and performance reconciled by design. *Proc. ACM Program. Lang.* **2018**, *2*, 120. [[CrossRef](#)]
45. Kwong, T. *Hands-On Design Patterns and Best Practices with Julia*; Packt Publishing: Birmingham, UK, 2020.
46. Fritzsche, S. Level structure and properties of open f -shell elements. *Atoms* **2022**, *10*, 7. [[CrossRef](#)]
47. Fritzsche, S.; Maiorova, A.V.; Wu, Z.W. Radiative recombination plasma rate coefficients for multiply charged ions. *Atoms* **2023**, *11*, 50. [[CrossRef](#)]
48. Fritzsche, S. Dielectronic recombination strengths and plasma rate coefficients of multiply charged ions. *Astron. Astrophys.* **2021**, *656*, A163. [[CrossRef](#)]
49. Fritzsche, S.; Surzhykov, A. Approximate atomic Green functions. *Molecules* **2021**, *26*, 2660. [[CrossRef](#)]
50. Fritzsche, S. Symbolic evaluation of expressions from Racah's algebra. *Symmetry* **2021**, *13*, 1558. [[CrossRef](#)]

51. Deprince, J.; Bautista, M.A.; Fritzsche, S.; Garcia, J.; Kallman, T.R.; Mendoza, C.; Palmeri, P.; Quinet, P. Plasma environment effects on K lines of astrophysical interest. I. Atomic structure, radiative rates, and Auger widths of oxygen ions. *Astron. Astrophys.* **2019**, *624*, A74. [[CrossRef](#)]
52. Haque, A.K.F.; Atiqur, M.; Patoary, R.; Uddin, M.A.; Basak, A.K.; Saha, B.C. Electron Impact Atomic and Ionic Ionization: Analytical, Semiempirical, and Semiclassical Methods. *Adv. Quantum Chem.* **2016**, *73*, 363. [[CrossRef](#)]
53. Donets, E.D.; Ovsyannikov, V.P. Investigation of ionization of positive ions by electron impact. *Zh. Eksp. Teor. Fiz.* **1981**, *80*, 916.
54. Colgan, J.; Fontes, C.J.; Zhang, H.L. Inner-shell electron-impact ionization of neutral atoms. *Phys. Rev. A* **2006**, *73*, 062711. [[CrossRef](#)]
55. Lecointre, J.; Jureta, J.J.; Defrance, P. Electron-impact ionization of singly-charged neon ions. *J. Phys. B* **2008**, *41*, 095204. [[CrossRef](#)]
56. Duponchelle, M.; Khouilid, M.; Oualim, E.M.; Zhang, H.; Defrance, P. Electron-impact ionization of neon ions ($q = 4-8$). *J. Phys. B* **1997**, *30*, 729. [[CrossRef](#)]
57. Tinschert, K.; Müller, A.; Hofmann, G.; Huber, K.; Becker, R.; Gregory, D.C.; Salzborn, E. Experimental cross sections for electron impact ionisation of hydrogen-like Li^{2+} ions. *J. Phys. B* **1989**, *22*, 531. [[CrossRef](#)]
58. Khouilid, M.; Cherkani-Hassani, S.; Rachafi, S.; Teng, H.; Defrance, P. Electron-impact single ionization of krypton ions ($q = 12-18$). *J. Phys. B* **2001**, *34*, 1727. [[CrossRef](#)]
59. Fritzsche, S.; Jiao, L.-G.; Wang, Y.-C.; Sienkiewicz, J.E. Collision Strengths of Astrophysical Interest for Multiply Charged Ions. *Atoms* **2023**, *11*, 80. [[CrossRef](#)]
60. Defrance, P. Recommended data for electron impact ionization of noble gas ions. *Nucl. Fusion Suppl.* **1995**, *6*, 43.
61. Blanke, J.H.; Fricke, B.; Finkbener, M. *Database Plasmarelevante Atomare Daten*; University of Kassel: Kassel, Germany, 1992.

Disclaimer/Publisher's Note: The statements, opinions and data contained in all publications are solely those of the individual author(s) and contributor(s) and not of MDPI and/or the editor(s). MDPI and/or the editor(s) disclaim responsibility for any injury to people or property resulting from any ideas, methods, instructions or products referred to in the content.